938Gb/s, 145-GHz-bandwidth Wireless Transmission Over the Air Using Combined Electronic and Photonic-assisted Signal Generation

Zichuan Zhou, Amany Kassem, James Seddon, Eric Sillekens,
Izzat Darwazeh, Polina Bayvel and Zhixin Liu
Department of Electronic & Electrical Engineering, University College London, United Kingdom
zichuan.zhou.14@ucl.ac.uk

Abstract— **We demonstrate an ultra-wide 145 GHz bandwidth wireless transmission of OFDM signals over the air spanning 5-150 GHz frequency region. This is achieved by combining the merits of high-speed electronics and microwave photonics technologies. The signals over 5-75 GHz are generated using high speed digital-to-analog converters. The high frequency mm-wave band signals, including W-band (75-110 GHz) and D-band (110-150 GHz) signals, are generated by mixing optically modulated signals with frequency-locked lasers on high-speed photodiodes. By frequency-locking two pairs of narrow linewidth lasers and refer the frequency difference to a common quartz oscillator source, we generated W-band and D-band signals with precise frequencies and significantly reduced phase noise compared to free-running laser counterpart, enabling enhanced spectral efficiency and utilization into W and D bands. The use of OFDM format and bit loading technique ensures 938 Gb/s capacity with minimal gaps between different RF and millimeter wave bands.**

***Keywords*—Data transmission, microwave photonics, millimeter, multi-band transmission, phase noise, frequency-division-multiplexing**

I. Introduction

The surge in new wireless, including HD-video streaming, AR/VR, and the Internet of Things, requires faster communication between devices and the Cloud. This has stimulated research in high-capacity mobile front-haul transmission, exceeding 100 Gb/s, using both analogue and digital radio-over-fiber technologies [1].

However, in deployed systems, many base stations are not connected to optical fibers. Instead, they use coaxial cables or wireless links to other base stations for communication with the Cloud. This has highlighted the need for high-capacity point-to-point wireless transmission between base stations to enhance the coverage and capacity of wireless networks, shown in Fig. 1.

To achieve this, multiple RF and mm-Wave frequency bands can be used simultaneously by deploying multiple transmitters (Tx) and receivers (Rx), resulting in multiband wireless transmission links [2,3]. Since the sub-6 GHz frequency band is heavily congested with existing wireless and mobile services like 4G and 5G, the high frequency RF bands (6-30 GHz) and some mm-wave bands and sub-TH (30-300 GHz) are of great interest for high-capacity future systems.

To date, the generation and transmission of these high-frequency signals has been achieved with both all-electronic and photonic-assisted techniques. Within the microwave and

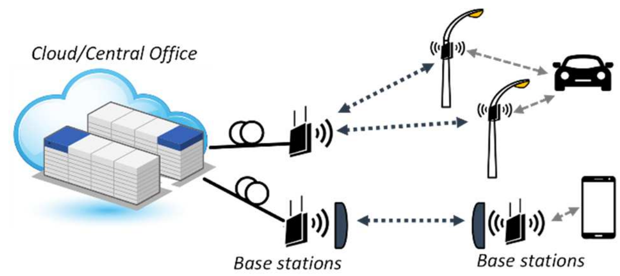

Fig.1: Wireless link connecting base stations.

low-mm wave regions, considerable work exists on developing RF and mm-wave components, including frequency synthesizers, detectors, and mixers. This has led to the demonstration of digital-to-analogue converters with bandwidth (BW) exceeding 80 GHz [4], digitizer with a 110-GHz BW [5], and mixers in the 110-170 GHz range [6]. While the all-electronic approach exhibits outstanding performance for signals below 80 GHz, it encounters hurdles in mm-wave signal generation, such as reduced power efficiency [6] and enhanced phase noise [7].

Conversely, photonics technologies show great promise in mm-wave and sub-THz carrier generation. By mixing optically modulated signals with a local oscillator (LO) laser on high-bandwidth photodiodes (PD), researchers have generated in W and D band signals, demonstrating 125 Gb/s at the W band in a single-in-single-out system [8], and 1.056 Tb/s using 24-GHz-BW using 4 pairs of dual-polarization TRx at D-band [9] (264 Gb/s each transmitter-receiver pair).

However, these demonstrations predominantly use free-running lasers for both signals and LO, which results in a random drift of the carrier frequencies of the generated mm-wave signals. This drift precludes the joint exploitation of both electronic and photonic-assisted signal generation methods in the generation and transmission of multiple closely spaced frequency bands.

In this paper, we harness both electronic and photonic methods to demonstrate a 145-GHz wireless ultra-wide-band transmission over the air, using a hybrid photonic-assisted and all-electronic transmission arrangement. This is achieved by combining three all-electronic channels, spanning frequencies from 5-50 GHz and 50-75 GHz, with two photonic-assisted wireless channels, covering W band (75-110 GHz) and D band (110-150 GHz). By frequency locking two pairs of lasers, we generated W-band and D-band signals with precise

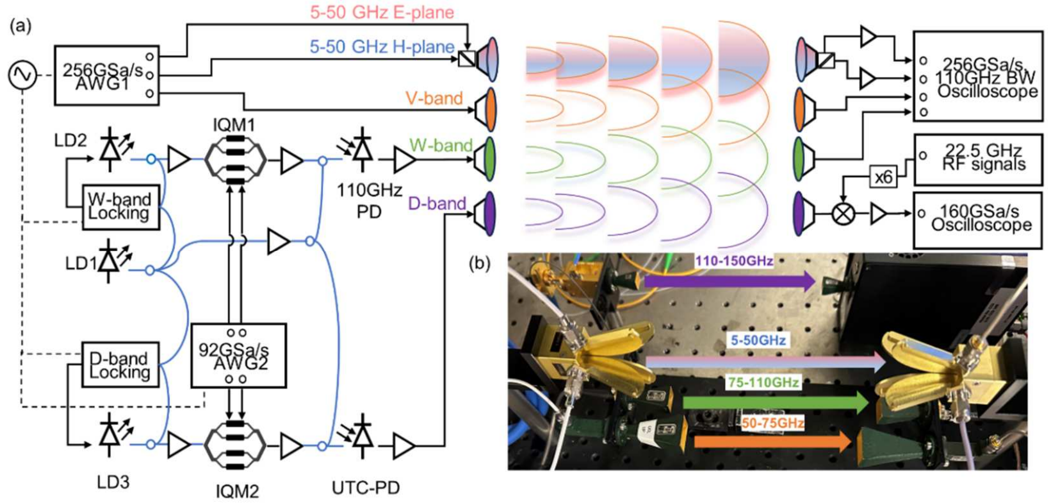

Fig. 2: Experimental setup. (a) system diagram, (b) photo of the transmission experiment. LD: laser diode; IQM: In-phase and Quadrature Modulator; PD: photodetector; AWG: Arbitrary Waveform Generator.

frequencies that referred to the same reference source as the all-electronic channels. Compared to demonstrations based on free-running lasers, our demonstrations using locked, narrow-linewidth signals have significantly improved phase noise for high spectral efficiency signal generation [10]. The mutual frequency locking eliminates the need for an ultra-stable cavity in conventional laser frequency stabilization methods [11], reducing system size and power consumption. Using bit-loaded orthogonal frequency division multiplexed (OFDM) signaling, we achieved 938 Gb/s capacity through a 12 cm non-collimated point-to-point wireless link. To the best of our knowledge, this is the highest BW wireless transmission link, potentially satisfying the high-capacity needs for point-to-point base station communications.

II. EXPERIMENTAL SETUP

Fig. 2a shows our experimental setup. At the transmitter side, three all-electronic channels are generated from an 80-GHz-BW 256-GSa/s arbitrary waveform generator (AWG1, Keysight M8199B) with 8 bits nominal resolution. Two of AWG1's output ports are connected to a dual-polarization quad-ridged horn antenna with 11-dBi gain to generate wireless OFDM signals over 5-50 GHz in two orthogonal polarizations, i.e., the E-plane and H-plane. A third output of AWG1 is used to drive a V-band horn antenna with 20-dBi gain to generate 50-75 GHz signals.

The OFDM signals are generated offline and upconverted digitally to an intermediate frequency (IF) of 27.5 GHz for the two-polarization multiplexed 5-50 GHz channels, and to an IF of 62.5 GHz for the 50-75 GHz channel. In all cases, the OFDM signals have 256 sub-carriers. Among them, 253 sub-carriers are each modulated using 16 quadrature amplitude modulation (QAM) format. Three subcarriers are sent unmodulated at the center and the low/high frequency edges. This yields subcarrier spacing of about 176 MHz for the polarization multiplexed 5-50 GHz channels and 97.7 MHz for the 50-75 GHz channel. The source data is from a pseudo-random binary sequence (PRBS) of length of 2^{17}-1. With a clipping ratio of 10 dB, the digital waveforms obtained have a peak-to-average-power ratio (PAPR) of 12 dB.

The two optically assisted bands are generated using three lasers, including an ultra-low linewidth laser (LD1, linewidth of 50 Hz), operating at 1554.82 nm, and two tunable lasers of 5 kHz (LD2) and 80 kHz (LD3) linewidth, both are frequency locked to LD1 with 92.5 and 130 GHz frequency offset using optical phase lock loop [12, 13]. The LD1 is tapped and split using polarization maintaining (PM) splitters before combining with the tapped continuous wave (CW) from LD2

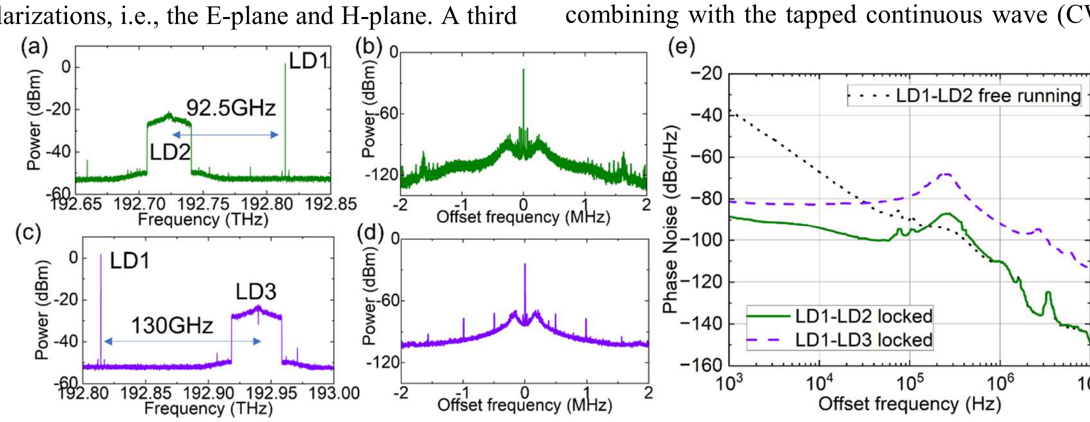

Fig. 3: Optical spectrum of (a) LD1-LD2 pair and (c) LD1-LD3 pair. Beat tone RF spectra of (b) LD1-LD2 pair and (d) LD1-LD3 pair and (e) Phase noise measurement of RF carrier generated with optically assisted technique.

and LD3 for frequency locking. The frequency locking was achieved by detecting the beat notes of the laser pairs and down converted to sub-50 MHz IF before being detected by phase frequency detectors (PFD) [14]. The outputs of the PFDs are fed to two proportional integral (PI) controllers to provide feedback signals that adjust the laser frequency through piezo-based tuning. We estimate a locking BW of about 100 kHz, limited by the BW of the piezo.

The CW outputs of LD2 and LD3 are amplified separately using PM erbium-doped fiber amplifier (EDFA) and modulated independently using two 40-GHz BW $LiNbO_3$ IQ modulators (IQM). Baseband waveforms of 17.5 GHz BW were used to drive IQM1 for the W-band signal generation, using the two synchronized outputs from a 92 GSa/s AWG with an analog BW of 25 GHz (AWG2, Keysight M8196a). Similarly, the D-band signals are generated IQM2 except for an increased signal BW of 20 GHz. The outputs of the IQMs are further amplified by PM-EDFAs to about 9 dBm before combining with the LD1 using PM couplers.

The W-band signal (75-110 GHz) is generated using a 110 GHz PD followed by a 110-GHz amplifier. The output of the amplifier is connected to a W-band horn antenna with 20 dBi gain. The D-band signal is generated by detecting the LD1-LD3 pair using a D-band uni-travelling-carrier (UTC) PD followed by a 110-170 GHz amplifier, before being transmitted using a 20-dBi horn antenna. This results in a 40 GHz BW OFDM signal spanning 110-150 GHz. The W and D band subcarrier spacing are 137 and 156 MHz.

At the receiver side, the sub-110 GHz channels are captured by three antennas of the same type as the transmitters side. The received signals are digitized by three analog-to-digital converters (ADC) on a 256 GSa/s 110-GHz BW real-time oscilloscope. The output of the D-band antenna is connected to a mm-wave mixer with an integrated ×6 frequency multiplier at the LO branch. Using a 22.5-GHz seed LO, the D-band signal is down converted to baseband before being digitized by a 160 GSa/s ADC. In principle, one can generate signals covering the full D-band with the UTC-PD. However, limited by the IF BW (17 GHz) of the mm-wave down-converter, we only detected the signals within the 135-150 GHz frequency region. Thus, the capacity of the transmitted signal in D band is limited by this IF BW.

The digitized signals in all five bands are processed offline using digital signal processing (DSP) including frequency domain pilot-based carrier recovery followed by one tap equalization [15, 16]. The bit loading [17] of each band is calculated based on the error vector magnitude of the signals, assuming 15.5% overhead soft-decision forward error of BER

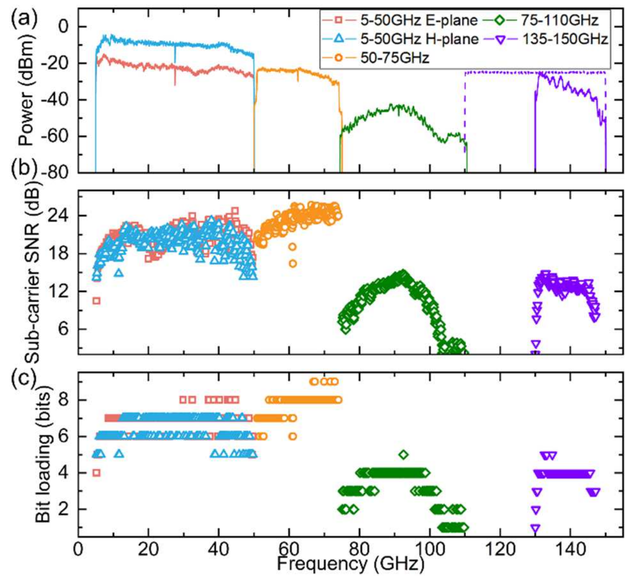

Fig. 4: Performance of the ultra-wide-band wireless transmission (a) spectra of the received signals, (b) SNR of the demodulated OFDM subcarriers, (c) bit loading of the subcarriers.

of 2.2e-2 [18]. We also transmitted the bit-loaded OFDM signals and measured the bit-error-ratio (BER) to validate the performance.

III. Experimental Results

A. Phase noise of locked laser pairs

Fig. 3a and 3c show the measured optical spectra of the modulated LD2 and LD3 with the same LO, with 92.5 GHz and 130 GHz spacing, respectively. Fig. 3b and 3d show the RF spectra of beat tones of LD1-LD2 and LD1-LD3 pairs, without modulation, showing a locking BW of about 100 kHz.

Fig. 3e shows the measured phase noise of the carrier signals generated by the frequency-locked LD1-LD2 pair (green solid curve) and LD1-LD3 pair (purple dashed curve), respectively. The black dotted curve shows the LD1-LD2 beat when the lasers are free running. By comparing black dotted and green solid curves, locked lasers show significant improvement of phase noise within the locking bandwidth (e.g., 50 dB improvement at 1 kHz). Compared to locked LD1-LD2, LD1-LD3 exhibits about 20dB higher phase noise across the entire measurement range, due to higher fundamental linewidth of the LD3. It has to be emphasized that carrier phase noise is only determined by laser phase noise and locking bandwidth, which is independent of frequency. By integrating the phase noise from 1 kHz to

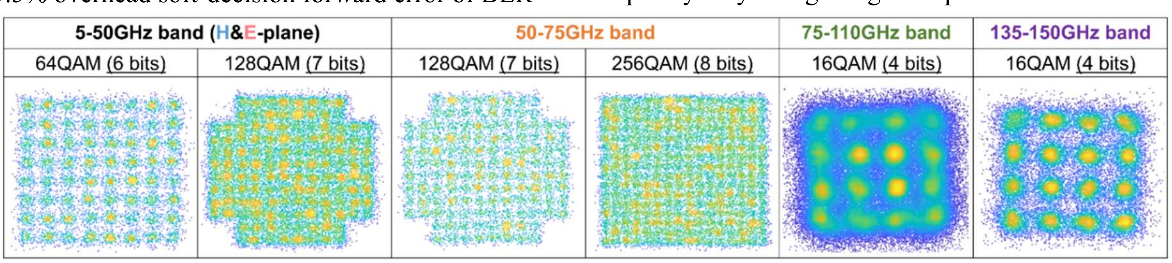

Fig. 5: Constellation diagrams of sub-carriers in different frequency bands, allocated with different modulation formats.

10 MHz, the estimated root-mean-square (rms) jitters of 92.5 and 130 GHz carrier are 46 and 278 fs, respectively. Again, the worse rms jitter of 130 GHz is limited by the linewidth of LD3. By replacing LD3 with LD2 for 130 GHz carrier generation, we expect reducing rms jitter to 33 fs.

B. Wireless transmission over 145GHz bandwidth

Fig. 4a shows the measured power spectrum of the received signals at a resolution of 100 MHz. The received 5-50 GHz H/E-plane, 50-75 GHz, 75-110 GHz and 135-150 GHz signals are shown by blue, pink, orange, green and purple solid curves respectively. Note that the transmitted signal in D band spans over the whole 110-150GHz region, as shown by the dashed purple line in Fig. 4a. For the 5-50 GHz signals, the H-plane signal has 10 dB higher power than the E-plane signal due to the higher receiver RF amplifier gain. Nevertheless, their signal-to-noise (SNR) are similar, showing an average SNR of 20.6 dB. This indicates that the signal quality is limited by the receiver's electronic noise. The V-band signal at 50-75 GHz shows a higher SNR, with an average SNR of 23.3 dB due to the higher antenna gain. The variation of signal power at different frequencies is due to the combined frequency response of the AWGs, the RF cables and the antennas. The W and D band signals have SNR of about 12 dB due to the relatively low transmitter amplifier gain and the higher link loss. With bit loading, each sub-carrier is allocated with the highest order of modulation formats that can achieve below 2e-2 BER, as plotted in Fig. 4c. The best-performing V-band subcarriers can mostly support 256 QAM, whilst the worst-performing D-band subcarriers mostly support 16 QAM. The estimated capacity using EVM-based bit-loading is 300, 285, 179, 106, and 68 Gb/s, for the E-plane, H-plane, V, W and D band signals, respectively. This results in an aggregated capacity of 938 Gb/s, corresponding to a net rate of 812 Gb/s. We note that the transmission distance is limited by the un-focused beams, which can be extended to >100 meters with lenses [9]. For illustration, Fig. 5 shows the constellation diagrams of sub-carriers at different frequency bands, classified by modulation format.

IV. Conclusion

We demonstrated a record-high BW wireless transmission using joint electronic and frequency-locked optical heterodyne methods, achieving a total of 145 GHz wireless transmission BW using five RF/mm wave bands (E/H-plane 5-50, 50-75, 75-110 and 110-150 GHz) with minimal frequency gap. The frequency-locked optical heterodyne technique enables improved RF carrier phase noise and spectrum utilization. The mutual frequency locking eliminates the need for a stable etalon in conventional laser frequency stabilization methods, leading to reduced cost and complexity. By using bit loaded OFDM format, a total aggregated 938 Gb/s data capacity has been achieved, corresponding to a net rate of 812 Gb/s. Our technology will benefit the high-capacity transmission needs between base stations.

Acknowledgment

Authors acknowledge the support from EPSRC ORBITS (EP/V051377/1), TRACCS(EP/W026252/1), TRANSNET (EP/R035342/1) and strategic equipment grant (EP/V007734/1).

References

[1] D. Che, "Analog vs Digital Radio-Over-Fiber: A Spectral Efficiency Debate From the SNR Perspective," J. Light. Technol, vol. 39, no. 16, 2021.

[2] A. Bekkali et al., "Multi-IF-Over-Fiber System With Adaptive Frequency Transmit Diversity for High Capacity Mobile Fronthaul," J. Light. Technol, vol. 37, no. 19, 2019.

[3] D. Nopchinda et al., "Experimental Demonstration of Multiband Comb-Enabled mm-Wave Transmission," IEEE Microw. Wireless Technol. Lett, vol. 33, no. 6, 2023.

[4] Keysight, "M8100 Arbitrary Waveform Generators,"https://www.keysight.com/gb/en/products/arbitrary-waveform-generators/m8100-series-arbitrary-waveform-generators.html, accessed Sep. 2023.

[5] Keysight, "Infiniium UXR-Series Oscilloscopes," https://www.keysight.com/gb/en/products/oscilloscopes/infiniium-real-time-oscilloscopes/infiniium-uxr-series-oscilloscopes.html, accessed Sep. 2023.

[6] C. J. Lee and C. S. Park, "A D-Band Gain-Boosted Current Bleeding Down-Conversion Mixer in 65 nm CMOS for Chip-to-Chip Communication," IEEE Microw. Wireless Comp. Lett, vol. 26, no. 2, 2016.

[7] J. Chen et al., "Does LO Noise Floor Limit Performance in Multi-Gigabit Millimeter-Wave Communication?," IEEE Microw. Wireless Comp. Lett, vol. 27, no. 8, 2017.

[8] Y. Cai et al., "Real-time 100-GbE fiber-wireless seamless integration system using an electromagnetic dual-polarized single-input single-output wireless link at the W band," Optics Lett, vol. 48, no. 4, 2023.

[9] X. Li et al., "1-Tb/s Millimeter-Wave Signal Wireless Delivery at D-Band," J. Light. Technol, vol. 37, no. 1, 2019.

[10] T. Xu and I. Darwazeh, "Identification and practical validation of spectrally efficient non-orthogonal frequency shaping waveform," Comm. Eng, vol. 2, no. 58, 2023.

[11] Z. Feng et al., "Comb-locked telecom-grade tunable laser using a low-cost FPGA-based lockbox," 2021 Conference on Lasers and Electro-Optics (CLEO), San Jose, USA, 2021, pp. 1-2.

[12] S. Ristic et al., "An Optical Phase-Locked Loop Photonic Integrated Circuit," J. Light. Technol, vol. 28, no. 4, 2010.

[13] K. Balakier et al., "Monolithically Integrated Optical Phase Lock Loop for Microwave Photonics," J. Light. Technol, vol. 32, no. 20, 2014.

[14] F. Friederich et al., "Phase locking of the beat signal of two distributed-feedback diode lasers to oscillators working in the MHz to THz range", Optics Exp., vol. 18, no. 8, 2010.

[15] Z. Liu et al., "Homodyne OFDM with Optical Injection Locking for Carrier Recovery," J. Light. Technol, vol. 33, no. 1, 2015.

[16] S. L. Jansen et al., "Coherent Optical 25.8-Gb/s OFDM Transmission Over 4160-km SSMF," J. Light. Technol, vol. 26, no. 1, 2008.

[17] A. M. Wyglinski et al., "Bit loading with BER-constraint for multicarrier systems," IEEE Trans. Wireless Comm, vol. 4, no. 4, 2005.

[18] T. Mizuochi et al., "Progress in soft-decision FEC," 2011 Optical Fiber Communication Conference (OFC), Los Angeles, USA, 2011, pp. 1-3.